Journal of Biomedical Optics

BiomedicalOptics.SPIEDigitalLibrary.org

Fluorescence lifetime imaging ophthalmoscopy in type 2 diabetic patients who have no signs of diabetic retinopathy

Dietrich Schweitzer
Lydia Deutsch
Matthias Klemm
Susanne Jentsch
Martin Hammer
Sven Peters
Jens Haueisen
Ulrich A. Müller
Jens Dawczynski

SPIE.

Fluorescence lifetime imaging ophthalmoscopy in type 2 diabetic patients who have no signs of diabetic retinopathy

Dietrich Schweitzer,[a,*] Lydia Deutsch,[a] Matthias Klemm,[b] Susanne Jentsch,[a] Martin Hammer,[a] Sven Peters,[a] Jens Haueisen,[b] Ulrich A. Müller,[c] and Jens Dawczynski[d]
[a]University Hospital Jena, Experimental Ophthalmology, Bachstrasse 18, D-07743 Jena, Germany
[b]Ilmenau University of Technology, Institute of Biomedical Engineering and Informatics, P.O. Box 100565, D-9868 Ilmenau, Germany
[c]University Hospital Jena, Clinic of Internal Medicine III, Erlanger Allee 101, D-07740 Jena, Germany
[d]University Hospital Leipzig, Department of Ophthalmology, Liebigstr.10–14, D-04103 Leipzig, Germany

Abstract. The time-resolved autofluorescence of the eye is used for the detection of metabolic alteration in diabetic patients who have no signs of diabetic retinopathy. One eye from 37 phakic and 11 pseudophakic patients with type 2 diabetes, and one eye from 25 phakic and 23 pseudophakic healthy subjects were included in the study. After a three-exponential fit of the decay of autofluorescence, histograms of lifetimes τ_i, amplitudes α_i, and relative contributions Q_i were statistically compared between corresponding groups in two spectral channels (490 < ch1 < 560 nm, 560 < ch2 < 700 nm). The change in single fluorophores was estimated by applying the Holm–Bonferroni method and by calculating differences in the sum histograms of lifetimes. Median and mean of the histograms of τ_2, τ_3, and α_3 in ch1 show the greatest differences between phakic diabetic patients and age-matched controls ($p < 0.000004$). The lack of pixels with a τ_2 of ~360 ps, the increased number of pixels with $\tau_2 > 450$ ps, and the shift of τ_3 from ~3000 to 3700 ps in ch1 of diabetic patients when compared with healthy subjects indicate an increased production of free flavin adenine dinucleotide, accumulation of advanced glycation end products (AGE), and, probably, a change from free to protein-bound reduced nicotinamide adenine dinucleotide at the fundus. AGE also accumulated in the crystalline lens. [DOI: 10.1117/1.JBO.20.6.061106]

Keywords: fluorescence lifetime imaging ophthalmoscopy; diabetes; metabolism; flavin adenine dinucleotide; reduced nicotinamide adenine dinucleotide; advanced glycation end products.

Paper 140774SSPR received Nov. 22, 2014; accepted for publication Feb. 16, 2015; published online Mar. 13, 2015.

1 Introduction

Detection of the earliest signs of diabetic retinopathy (DR) increases the probability of reducing further pathological developments, provided that an appropriate therapy will be administered.[1,2]

Apoptosis of vascular and neural cells has been reported for the early onset of DR.[3] Furthermore, in diabetes, neuronal degeneration due to apoptosis in the inner retina has been found to be 10-fold higher than that in vascular cells.[4,5]

Barber et al.[3] found that apoptosis of neural cells is an earlier marker than is damage of vascular cells. No change in concentration of reduced nicotinamide adenine dinucleotide (NADH) was found between excited retina of diabetic rats and controls.[6] Further studies were performed on excited retinas of rats under euglycemic and hyperglycemic conditions as well as *in vivo* on diabetic rats.[7] In these studies, no elevated cytosolic NADH/NAD ratio was found under hypoglycemic conditions nor in diabetes, both *in vitro* and *in vivo*. But they found an increased polyol synthesis and metabolites upstream of glucose like the sorbitol pathway, which decreases NADPH.

Increased oxidation of sorbitol results in the generation of cytosolic NADH, which in early diabetes leads to metabolic imbalance as well as neural and vascular damage.[8]

In diabetic rats that were provided with a low dose of insulin, the thicknesses of the inner nuclear and plexiform layers were significantly reduced after 7.5 months. The density of ganglion cells was also reduced. These neurodegenerative changes were observed in the absence of morphologic vascular changes.[9]

Spectral domain optical coherence tomography showed that the total thickness of the retinal layer, particularly the retinal nerve fiber layer, was significantly thinner in diabetic Otsuka Long-Evans Tokushima fatty rats after 28 weeks than in non-diabetic Long-Evans Tokushima Otsuka rats. Additionally, a decreased number of ganglion cells and an increased frequency of apoptosis have been found by histological investigations.[10]

Isolated retinal capillary cells showed typical signs of mitochondrial dysfunction, including an increased release of cytochrome c into the cytosol and an accumulation of the proapoptotic protein Bax in mitochondria cells when incubated in 20 mM glucose. However, these changes were inhibited in the presence of superoxide dismutase.[11]

In diabetic patients, first metabolic alterations were found by Field et al.[12] They excited the fundus using flashes of 467 nm light in a 3-deg field and detected the autofluorescence at 535 nm.

*Address all correspondence to: Dietrich Schweitzer, E-mail: dietrichschweitzer@googlemail.com

Increased fluorescence intensity and a wider distribution of intensity of all pixels in the excited field were found in diabetic patients in relation to controls. These results were interpreted as the result of an impaired electron transport by energy-generating enzymes in the respiratory chain. Because of the specific excitation and emission wavelengths, an increased contribution of flavin adenine dinucleotide (FAD) was assumed.

The problem of *in vivo* fluorescence measurement is that the crystalline lens and the fundus layers are simultaneously excited. An exact interpretation of the spectrally resolved fundus fluorescence is possible only in eyes with artificial intraocular lenses (IOL) or when the fluorescence of the crystalline lens is separately detected and subtracted from the fluorescence of the whole eye.[13,14]

In clinical practice, the classification of DR is based on vascular changes according to the Early Treatment Diabetic Retinopathy Study Research Group.[15]

Using the highly accurate spectral domain optical coherence tomography, it was demonstrated that the thicknesses of the retinal nerve fiber layer, the ganglion cell layer, and the inner plexiform layer were reduced in patients with minimal signs of DR in the pericentral macular area compared with those in the controls. Moreover, in the peripheral macular area, the retinal nerve fiber layer and the inner plexiform layer were found to be thinner than in the controls. The DR status was the only significant explanatory variable for this reduced thickness.[16]

Measurements of the time-resolved fluorescence of endogenous fluorophores have the potential to detect metabolic alterations in the human fundus.[17] The redox pairs of oxidized and reduced NAD-NADH and FAD-$FADH_2$ act as electron carriers in the basic processes of energy metabolism (citrate acid cycle, respiratory chain). Additional fluorophores, such as lipofucin components, advanced glycation end products (AGE), collagens, elastin, products of the visual cycle (retinol), or components of heme synthesis (protoporphyrin IX), contribute to the autofluorescence of the fundus. In principle, these fluorophores can be discriminated by measuring specific excitation and emission spectra. Due to the transmission of the ocular media, however, excitation of endogenous fluorophores is only possible for wavelengths longer than 400 nm. Because the excitation maxima of most of these fluorophores are at wavelengths shorter than this value, any discrimination based on excitation spectra is difficult. The decay of fluorescence intensity (lifetime) after pulse excitation permits the differentiation of fluorophores with overlapping emission spectra. The free or protein-bound status of a fluorophore can also be distinguished if the emission spectrum is equal in both cases.

The excitation and emission spectra and the lifetimes of the expected fundus fluorophores and of the anatomical structures of porcine eyes have been reported.[18]

The purpose of this study was to determine whether metabolic changes in the time-resolved autofluorescence of the fundus are detectable in diabetic patients who have no signs of DR.

2 Participants and Methods

2.1 *Participants*

The patients were recruited from the outpatient Clinic of Internal Medicine III of the Jena University Hospital. Inclusion criteria were a diagnosis of type 2 diabetes, no signs of DR, and no or minimal cataracts. No subject was suffering from posterior capsule opacification. The DR stage was blindly evaluated from color fundus images by a retina specialist. The subjects in the control group were volunteers or patients from the Eye Clinic of the Jena University Hospital and did not have diabetes mellitus. They had no ocular disease and had clear media or a mild cataract (nuclear or cortical stadium 1).[19] Subjects suffering from systemic diseases that could influence ocular metabolism were not included. Because the fluorescence decay depends on age,[20,21] the only subjects who were included in the age-matched comparison between diabetic patients who have no signs of DR and healthy subjects were older than 40 years. The investigation was performed predominantly on subjects with a crystalline lens. For comparison, small groups of pseudophakic (IOL) diabetic patients and healthy subjects were investigated.

All subjects provided written consent to participate in the study. All research procedures were performed according to the Declaration of Helsinki. Approval for the study was obtained from the ethics committee of the Jena University Hospital.

HbA1c was measured using high-performance liquid chromatography (official normal range 4.4% to 5.9%; mean 5.2; TOSOH-Glykohämoglobin-Analyzer-HLC-723-GHbV; Tosoh, Tokyo, Japan). The mean normal range measured in 1079 nondiabetic patients in 2009 was $5.65\% \pm 0.38\%$.[22] Therefore, we adjusted the HbA1c according to the mean normal value of healthy people to the value of 5.05% (32 mmol/mol) that was found in the Diabetes Control and Complication Trial Research Group (DCCT).[23] Blood pressure was measured immediately before the autofluorescence measurement. Table 1 shows the data of the subjects who were included in the study. Values are given as the mean $\pm$ standard deviation.

The albumin/creatinine ratio in the urine indicates that some diabetic patients were suffering from microalbuminuria, and some were partly already suffering from macroalbuminuria. Microalbuminuria is assumed for albumin/creatinine ratios of 30 to 300 mg/g, and macroalbuminuria is present for ratios >300 mg/g.

2.2 *Measuring System*

The time-resolved autofluorescence of the fundus was measured using a modified confocal scanning laser ophthalmoscope (HRA II, Heidelberg Engineering GmbH, Heidelberg, Germany). The optomechanical unit of an HRA II was modified at the Eye Clinic of the University of Jena, Germany, for fundus excitation by a pulsed laser (BDL-440-SMC, Becker&Hickl GmbH, Berlin, Germany), which emitted 75-ps pulses at 448 nm at an 80 MHz repetition rate.[18] The fluorescence was detected in two spectral channels (ch1: 490 to 560 nm, ch2: 560 to 700 nm) using multichannel plate photomultipliers (Ham-R 3809U-50, Hamamatsu, Herrsching, Germany). The fluorescence decay was detected using time-correlated single photon counting (TCSPC) by an SPC 150 board (Becker&Hickl GmbH). An HRT 41 router (Becker&Hickl GmbH) separated the photons from the two spectral channels. Fluorescence decay images were recorded from a 30-deg field with a resolution of $\sim 40 \times 40\ \mu m^2$. The excitation power was 100 μW in the cornea plane. Simultaneously with the excitation laser, the fundus was illuminated with an infrared laser (820 nm), which provided contrast-rich fundus images for automatic image registration in both spectral channels. This device was the forerunner model of the demonstrator developed by Heidelberg Engineering.[21]

Table 1 Characterization of the subjects included in the study.

	Diabetes type 2		Healthy subjects	
	Crystalline lens	IOL	Crystalline lens	IOL
Probands	37	11	25	23
Age (years)	60.5 ± 15.3	61.1 ± 14.7	61.9 ± 17.3	65.3 ± 14.7
Gender	22 M, 15 F	8 M, 3 F	14 M, 11 F	10 M, 13 F
BMI (kg/m^2)	29.8 ± 6.1	30 ± 6	26.6 ± 4.2	26.7 ± 4
Systolic blood pressure (mmHg)	138.9 ± 15.4	136.4 ± 16.5	134.8 ± 12.2	135.1 ± 12.4
Diastolic blood pressure (mmHg)	82.3 ± 10.8	81.5 ± 10	78.9 ± 8.8	78.1 ± 9
Antihypertonic drugs	81	100	28	39
Statins (%)	43	70	8	13
Time since diagnosis of diabetes (years)	14.7 ± 9.8	16.4 ± 10.7		
Oral antihyperglycemic agents (%)	30	20		
Treatment with insulin	57	60		
Diet (%)	13	20		
HbA1C DCCT adjusted (mmol/mol; %)	49.9 ± 13.9; 7.1 ± 1.4	46.3 ± 7.6; 6.8 ± 0.7		
Neuropathy (%)	24	20		
Albumin/creatinine in urine (mg/g)	76 ± 233	154 ± 198		
Albumin/creatinine in urine >20 mg/g (% patients)	27	30		

Note: IOL, intraocular artificial lens.

2.3 *Fitting of the Fluorescence Decay*

The software SPCImage3.6 (Becker&Hickl GmbH) was used to evaluate the time-resolved autofluorescence images. To obtain a sufficient number of photons, a binning factor B = 2 was used, which increased the number of photons at a single pixel by a factor of 25. The fluorescence decay was approximated by the three-exponential model function given in Eq. (1):

$$I(t) = \mathrm{IRF} \times \sum_{i=1}^{3} a_i \cdot e^{-\frac{t}{\tau_i}} + b, \tag{1}$$

where $I(t)$ is the number of photons at time t, IRF is the instrument response function, a_i is the amplitude or pre-exponential factor, τ_i is the lifetime of exponent i, and b is the background.

To avoid the influence of the stepped slope of fluorescence intensity which is caused by the fluorescence of the crystalline lens, a tailfit was employed.

The criterion for an optimal approximation was the minimization of χ_r^2 [Eq. (2)]:

$$\chi_r^2 = \frac{1}{n-q} \cdot \sum_{j=1}^{n} \frac{[N(t_j) - N_c(t_j)]^2}{N(t_j)}, \tag{2}$$

where n represents the time channels (1024 applied here), q represents the free parameters (α_i, τ_i, and b), $N(t_j)$ represents the detected photons in time channel j, and $N_c(t_j)$ represents the photons from the convolution of the model function with the IRF.

Assuming that the detection of photons is a Poisson process, the limiting value in Eq. (2) is 1.

In addition to all of the individual amplitudes and lifetimes, the mean lifetime τ_m and the relative contribution Q_i parameters are important for evaluating fluorescence lifetime imaging ophthalmoscopy (FLIO) measurements. Here, the mean lifetime is defined as

$$\tau_m = \frac{\sum_{i=1}^{p} \alpha_i \cdot \tau_i}{\sum_{i=1}^{p} \alpha_i}. \tag{3}$$

The relative contribution Q_i of the component i corresponds to its respective area under the decay curve.

$$Q_i = \frac{\alpha_i \cdot \tau_i}{\sum_{i=1}^{p} \alpha_i \cdot \tau_i}. \tag{4}$$

Pixel-by-pixel fitting of the measured fluorescence decay to a three-exponential model [Eq. (1)] results in images of the lifetimes τ_1, τ_2, and τ_3, and the amplitudes α_1, α_2, and α_3 for the fundus of each subject in both channels. Images of τ_m and of Q_i can be calculated from the lifetimes and amplitudes.

Because the system did not contain an internal fixation target, the 30-deg field was not exactly at the same position at the fundus for all subjects. Thus, the comparison of the FLIO parameter of the complete images was not appropriate. Therefore, after approximation of the fluorescence decay of each pixel of the whole image, a region of interest (RoI) of 71×101 pixels, which was located in the superior temporal quadrant that

included the macula, was selected for further calculations in all measurements. This region was contained in all images.

2.4 *Evaluation of Fitting Results*

In our study, we calculated the fitting results for each pixel within the RoI (71×101 pixels) and determined how frequently each value was determined for each lifetime τ_i, amplitudes α_i, and Q_i. In this way, one histogram of each τ_i, α_i, and Q_i was calculated in both spectral channels for each subject. The histograms of phakic diabetic patients and healthy subjects were compared in two steps.

First, the derived quantities' mode, mean, and median from these histograms were compared for each individual between the two groups. The statistical comparison was performed using SPSS 21 (IBM Deutschland GmbH, Ehningen, Germany). The two-tailed t test was used if the error probability in the Kolmogorov-Smirnov test was >0.2 (normal distribution). Equality of variances was assumed if the error probability in the Levene-test was also >0.2. The Mann-Whitney U test was used if the parameters were not normally distributed. Significant differences in the fitting parameters were assumed for $p < 0.05$. The area under curve of the receiver operating characteristics (ROC) was calculated. The ideal value is 1, while a value of 0.5 indicates that the separation between groups is only stochastic. Sensitivity and specificity were given for ROC > 0.72. These results are global because each lifetime τ_i and amplitude α_i results from the sum of the contributions from several fluorophores.

In a second step, changes in the single fluorophores were estimated. For this process, the Holm–Bonferroni method[24] was applied using the software program FLIMX, which was developed at the University of Ilmenau.[25,26]

Here, the distribution of each fit parameter was divided into n intervals. The lifetimes in such intervals are, to a certain degree, determined by specific fluorophores. Differences between the fitting parameters in single intervals are considered significant if the error probability p is lower than the significance level α divided by the number n of intervals. The Wilcoxon test was performed for statistical comparison of the fit parameters of diabetic patients and healthy subjects in each interval.

The crystalline lens has a long fluorescence lifetime which influences the FLIO parameters, especially in channel 1. In contrast, an artificial IOL exhibits no fluorescence.

For that reason, the range of fit parameters was different for subjects with crystalline lens and for pseudophakic subjects. The size of the intervals was iteratively determined until the sum of the sensitivity and of specificity as well as ROC was maximal. The ranges and the size of the intervals for the fitting parameters are given in Table 2 for phakic subjects and in Table 3 for pseudophakic subjects.

3 Results

The decay of the fluorescence intensity was fitted by the three-exponential model function of Eq. (1) for each pixel in both spectral channels. As demonstrated in Fig. 1, the model function sufficiently approximates the measured decay.

After the fitting, images of the lifetimes, amplitudes, and relative contributions were calculated for both spectral channels. Figure 2 shows these images in the short-wavelength channel for a healthy subject and for a patient with diabetes but no signs of DR. The bluer color in the images of the patient with diabetes indicates a prolongation of the lifetimes.

Table 2 Range of fitting parameters for phakic subjects.

Parameter	Interval size	Range ch1	Range ch2
α_1 in %	2	74 to 92	60 to 88
α_2 in %	1	8 to 19	14 to 34
α_1 in %	0.5	1 to 6.5	1.5 to 5
τ_1 in ps	5	35 to 105	45 to 105
τ_2 in ps	10	330 to 690	300 to 590
τ_3 in ps	50	2500 to 4600	1800 to 3500
τ_m in ps	10	120 to 370	150 to 360
Q_1 in %	2	12 to 36	9 to 35
Q_2 in %	1	13 to 37	30 to 47
Q_3 in %	2	26 to 74	20 to 50

Table 3 Range of fitting parameters for pseudophakic subjects.

Parameter	Interval size	Range ch1	Range ch2
α_1 in %	2	72 to 90	60 to 80
α_2 in %	1	10 to 24	18 to 29
α_1 in %	0.5	0.5 to 5	2 to 6
τ_1 in ps	5	45 to 85	45 to 85
τ_2 in ps	10	330 to 460	330 to 460
τ_3 in ps	50	2000 to 3000	1800 to 2300
τ_m in ps	10	100 to 250	160 to 270
Q_1 in %	2	19 to 41	12 to 34
Q_2 in %	1	28 to 45	38 to 49
Q_3 in %	2	22 to 46	22 to 46

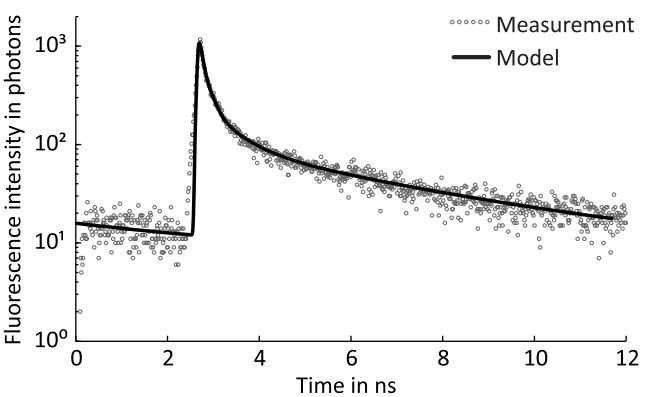

Fig. 1 Tailfit of a paramacular pixel by a three-exponential model function. The fit parameters are $\alpha_1 = 82.3\%$, $\alpha_2 = 11.3\%$, $\alpha_3 = 6.4\%$, $\tau_1 = 105$ ps, $\tau_2 = 639.8$ ps, $\tau_3 = 4294.4$ ps, and $\chi_r^2 = 1.14$.

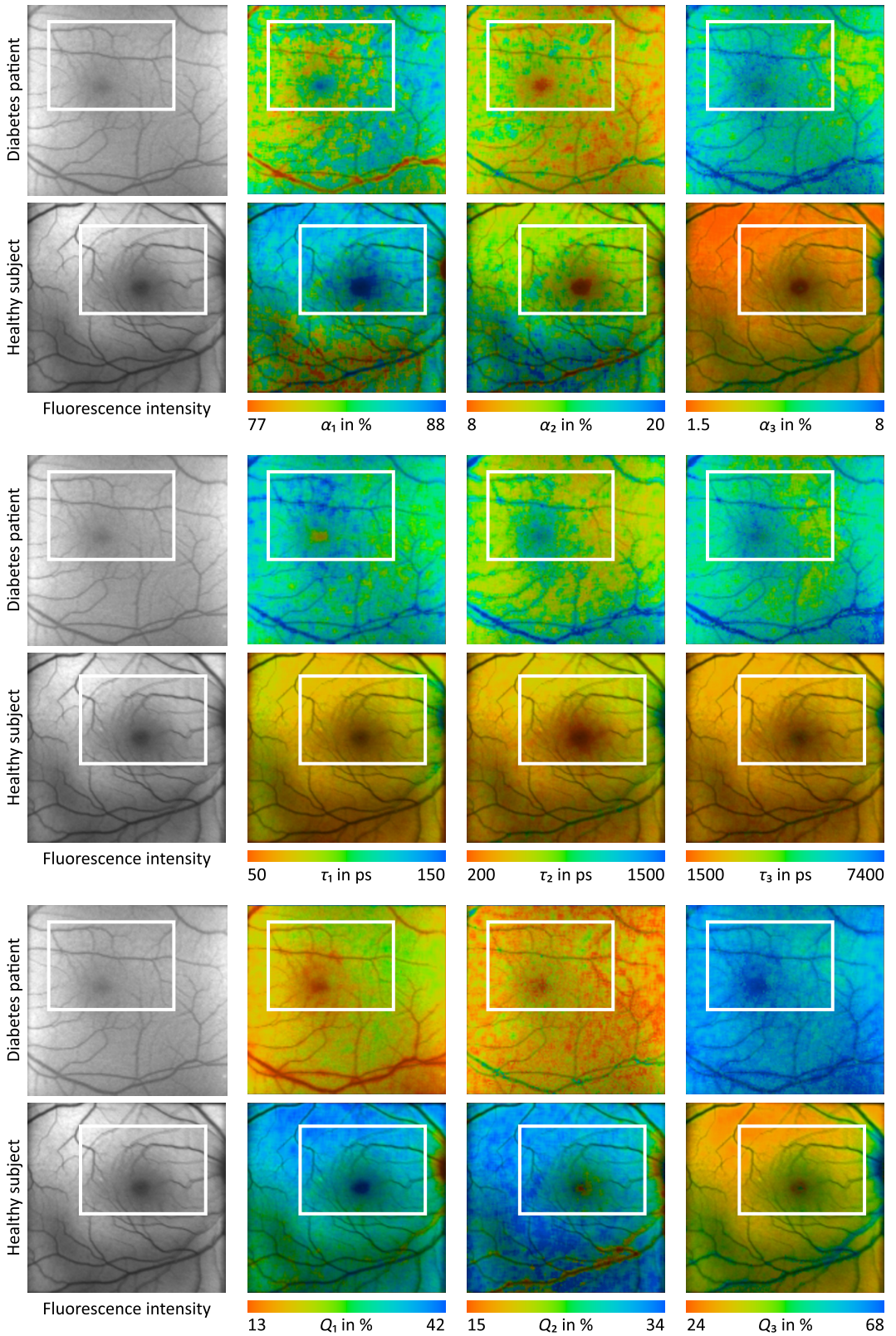

Fig. 2 Paired comparison of the amplitudes α_i (upper two rows of images), lifetimes τ_i (middle two rows of image), and relative contributions Q_i (lower two rows) of a diabetic patient and a healthy subject in the short-wavelength channel. Images of the diabetic patients are in the upper part, and images of the healthy subject are in the lower part of each double row of images. The regions of interest are highlighted (white box).

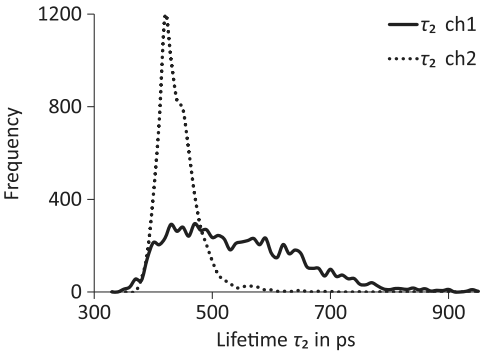

Fig. 3 Histograms of lifetime τ_2 of 7171 pixels in channels 1 and 2. The statistical parameters in picoseconds are as follows: for ch1: mode = 470, median = 549, mean = 528, standard deviation = 134; for ch 2: mode = 420, median = 442, mean = 435, standard deviation = 36.4.

The size and the position of the ROIs selected for quantitative comparison of the histograms of FLIO parameters are also shown in Fig. 2.

Generally, each histogram shows how often the same value of each parameter (lifetime, amplitude, and relative contribution) was determined in the analyzed field of a subject.

Figure 3, as an example, depicts the histogram of the lifetime τ_2 of a diabetic patient in ch1 and ch2. The differences in the distribution of the lifetime τ_2 in the two spectral channels indicate that the fluorescence results from different substances. Furthermore, this difference was detected equally in both the diabetic patients and the healthy subjects. From these distributions, statistical parameters were extracted for each subject.

The results of the statistical comparison are given for subjects with a crystalline lens in Table 4 for channel 1 (490 to 560 nm) and in Table 5 for channel 2 (560 to 700 nm).

In the short-wavelength channel, the best discrimination between healthy subjects and diabetic patients who have no signs of DR was achieved for the median and mean parameters in the distributions of α_3, τ_2, τ_3, τ_m, Q_1, Q_2, and Q_3. The statistical values of skewness and kurtosis mostly did not reach significance. The highest ROC value (0.875) with 83.8% sensitivity and 76% specificity was found for the median of τ_2 in ch1 with an error probability $p = 0.000001$. Good discrimination was also achieved for the medians of α_3 and τ_3 in the short-wavelength channel with error probabilities of $p = 0.000005$.

No significant difference between the two groups was obtained for the amplitude α_2. In contrast, the difference in the lifetime τ_2 between the two groups is highly significant, supporting the assumption that the composition of the fluorescent substances changes.

The best discrimination was obtained in the long-wavelength channel (560 to 700 nm) using the median and mean of the distributions of τ_2, τ_3, Q_1, Q_2, and Q_3 in the selected RoIs at the fundus (Table 5).

The statistical comparison was also performed for pseudophakic patients and controls (Table 6). Only 10 subjects were included in the diabetic group; thus, the value of the statistical comparison is limited. The median and mean were only significantly different for τ_2 in the short-wavelength channel, but on a much lower level than in phakic eyes. Surprisingly, the best discrimination was possible for the kurtosis of the amplitude α_3. In the long-wavelength channel, the differences for the median and mean reached significance for τ_1 and τ_3.

Figure 4 shows median boxplots for all FLIO parameters in ch1 and ch2 for phakic subjects. For pseudophakic subjects, only significantly different parameters are given.

To obtain more information about the substance-specific changes in the eyes of diabetic patients as an early sign of metabolic alterations before the signs of DR are visible, the Holm–Bonferroni test was applied. Many fluorophores are excited in the eye. Thus, each lifetime τ_i in a three-exponential approximation includes lifetimes from different fluorophores. Thus, the histograms that are created from the fitting parameters for all of the RoI pixels reflect the contributions of several fluorophores.

Therefore, similar to each approximated τ_i, the contribution of individual fluorophores with slightly different lifetimes can be estimated if the range of τ_i is divided into intervals. In each interval, the difference in each fitting parameter was tested between the distributions corresponding to healthy subjects and diabetic patients. The discriminations between the groups are independent of the intervals; thus, the results of intervals with high sensitivity and high specificity can be combined to obtain the best separation. Table 7 summarizes the results of the Holm–Bonferroni test for phakic diabetic patients and healthy subjects.

The best discrimination between healthy subjects and diabetic patients who have no signs of DR was obtained for the lifetime τ_2 in ch1 (490 to 560 nm) in the interval of 400 to 410 ps (ROC = 86%, sensitivity = 83.8%, specificity = 84%), τ_3 for 3050 ps in the interval 2800–3100 ps (ROC = 84%, sensitivity = 75.7%, specificity = 86%), and Q_2 for 29% (ROC = 85%, sensitivity = 89.2%, specificity = 72%).

In the long-wavelength channel, the best separations were found for τ_3 at 2100 ps (ROC = 85%, sensitivity = 89.2%, specificity = 80%) and for Q_2 at 43% (ROC = 87%, sensitivity = 75.7%, specificity = 96%).

In the comparison between the controls and the diabetic patients with an artificial IOL, significance in the Holm–Bonferroni test was only reached for τ_1 at 65 ps (ROC = 81%, sensitivity = 80%, specificity = 69.6%) in ch1 (Table 8). The intervals of the fitting parameters are given for the parameters whose ROC values are at least 0.7. We speculate that the low number of diabetic patients with an artificial IOL led to the lower number of significant parameters compared with the results in Table 7. On the other hand, these results point at the considerable influence of changes in the fluorescence of diabetic lenses.

Graphical analysis of the histograms is a further step in the interpretation of metabolic alterations at the fundus of diabetic patients. The sum and difference histograms of τ_2 in ch1 for diabetic patients and for healthy subjects with a crystalline lens are given in Fig. 5.

We observe a shift in the sum histograms for τ_2 to longer fluorescence decay times in the fundus of diabetic patients who show no signs of DR compared with those for the controls. The curve in the difference histogram of τ_2 in Fig. 5 clearly shows that in the RoI of diabetic patients, the number of pixels with a decay time of ~380 ps is reduced, whereas more pixels with fluorescence decay times longer than ~450 ps are present compared with those in the controls.

As demonstrated in Fig. 6, there is also a shift in the sum histograms of τ_3 to longer fluorescence decay times in the fundus of diabetic patients who show no signs of DR when compared with the controls.

Table 4 Statistical comparison based on the fit parameters of the fundus fluorescence in channel 1 (490 to 560 nm) for the phakic eyes of healthy subjects and diabetic patients who have no signs of diabetic retinopathy (DR).

Fit parameter		Test	Modal	Median	Mean	SD	Skewness	Kurtosis
Channel 450 to 560 nm	α_1	*t* test		0.008	0.011	ns	ns	
		Mann-Whitney	0.013					0.003
	α_3	*t* test		1E-06	1E-06			
		Mann-Whitney	8E-05			2E-05	ns	ns
		ROC	0.829	0.842	0.845	0.827	ns	ns
		Sensitivity	0.892	0.81	0.8	0.76		
		Specificity	0.72	0.72	0.845	0.824		
	τ_1	*t* test		0.004	0.008			
		Mann-Whitney	0.036			0.024	0.008	ns
	τ_2	Mann-Whitney	1E-06	1E-06	1E-06	3E-06	ns	ns
		ROC	0.862	0.875	0.875	0.854		
		Sensitivity	0.784	0.838	0.946	0.838		
		Specificity	0.8	0.76	0.72	0.72		
	τ_3	*t* test		4E-06	4E-06		ns	ns
		Mann-Whitney	0.001			5E-05		
		ROC		0.837	0.837	0.808		
		Sensitivity		0.83	0.837	0.73		
		Specificity		0.76	0.76	0.8		
	τ_m	*t* test		3E-06	3E-06		ns	
		Mann-Whitney	6E-05			2E-05		0.024
		ROC	0.803	0.837	0.837	0.826		
		Sensitivity	0.73	0.73	0.73	0.73		
		Specificity	0.76	0.84	0.84	0.72		
	Q_1	*t* test		1E-06	3E-06	ns	ns	
		Mann-Whitney	6E-05					0.018
		ROC	0.781	0.827	0.829			
		Sensitivity	0.72	0.72	0.72			
		Specificity	0.703	0.757	0.784			
	Q_2	*t* test		1E-07	1E-07	ns	ns	ns
		Mann-Whitney	1E-05					
		ROC	0.822	0.848	0.848			
		Sensitivity	0.72	0.76	0.76			
		Specificity	0.757	0.838	0.811			
	Q_3	*t* test	ns	1E-07	1E-07	ns	0.029	ns
		ROC		0.85	0.852			
		Sensitivity		0.865	0.865			
		Specificity		0.72	0.72			

Note: ns, nonsignificant; ROC, receiver operating characteristic.

Table 5 Statistical comparison based on the fit parameters of the fundus fluorescence in channel 2 (560 to 700 nm) for the phakic eyes of healthy subjects and diabetic patients who have no signs of DR.

Fit parameter		Test	Modal	Median	Mean	SD	Skewness	Kurtosis
Channel 560 to 700 nm	α_3	*t* test		0.004	0.004		ns	
		Mann-Whitney	0.003			0.001		0.004
	τ_1	*t* test		0.022	0.038	0.018	ns	ns
		Mann-Whitney	0.0005					
		ROC	0.724	0.735	0.746	0.75		
		Sensitivity	0.81	0.838	0.784	0.757		
		Specificity	0.6	0.64	0.64	0.72		
	τ_2	*t* test		8E-05	9E-05	0.001		
		Mann-Whitney	0.0001				0.008	0.018
		ROC	0.783	0.798	0.791	0.776		
		Sensitivity	0.757	0.78	0.757	0.757		
		Specificity	0.72	0.64	0.73	0.76		
	τ_3	*t* test	1E-06	2E-05	2E-05	2E-05	ns	ns
		ROC	0.84	0.841	0.845	0.81		
		Sensitivity	0.784	0.811	0.811	0.73		
		Specificity	0.76	0.76	0.76	0.68		
	τ_m	*t* test	0.001	0.001	0.001		ns	
		Mann-Whitney				0.008		0.041
		ROC	0.746	0.762	0.759			
		Sensitivity	0.703	0.703	0.703			
		Specificity	0.6	0.64	0.64			
	Q_1	*t* test		0.005	0.005	3E-05	ns	0.001
		Mann-Whitney	0.016					
		ROC				0.815		0.777
		Sensitivity				0.76		0.68
		Specificity				0.703		0.785
	Q_2	*t* test	1E-07		7E-05	0.001	ns	ns
		Mann-Whitney		3E-06				
		ROC	0.872	0.851	0.857	0.734		
		Sensitivity	0.76	0.8	0.84	0.56		
		Specificity	0.919	0.757	0.73	0.676		
	Q_3	*t* test	4E-05	6E-05	6E-05	5E-06	ns	ns
		ROC	0.791	0.794	0.794	0.83		
		Sensitivity	0.73	0.703	0.838	0.757		
		Specificity	0.68	0.76	0.68	0.72		

Table 6 Statistical comparison based on the fit parameters of the fundus fluorescence of the pseudophakic eyes of healthy subjects and diabetic patients who have no signs of DR.

Fit parameter		Test	Modal	Median	Mean	SD	Skewness	Kurtosis
Channel 490 to 560 nm	α_3	Mann-Whitney	ns	ns	ns	ns	ns	0.007
		ROC						0.796
		Sensitivity						0.739
		Specificity						0.7
	τ_2	*t* test	ns	0.042	0.031	ns	ns	ns
	τ_3	*t* test	0.031	ns	ns	ns	0.047	ns
	τ_m	*t* test	0.035	ns	ns	ns	ns	
		Mann-Whitney						0.028
	Q_3	*t* test	ns		ns	ns	0.036	ns
		Mann-Whitney		0.04				
Channel 560 to 700 nm	α_3	Mann-Whitney	ns	ns	ns	ns	ns	0.042
	τ_1	*t* test	ns	0.017	0.014	ns	ns	ns
	τ_3	Mann-Whitney	ns	0.038	0.028	ns	ns	ns
	Q_2	Mann-Whitney	ns	ns	ns	ns	ns	0.02

Likewise, considering the difference histogram for the decay time τ_3 in Fig. 6, fewer pixels with a lifetime of ~3000 ps are present in diabetes, and more pixels with longer decay times of ~3900 ps are present in the selected RoIs.

Longer decay times for τ_2 and τ_3 in the short-wavelength channel as well as higher values of α_3 were observed in the diabetic patients versus controls.

4 Discussion

The detection of early metabolic changes in the fundus is important for the development of a specific treatment for DR. First *in vivo* spectral measurements of metabolic alterations at the fundus of diabetic patients were published by Field et al.[12] It is assumed that alterations in the retinal vessel system[3] or thinning of fundus layers[16] are most likely consequences of metabolic malfunction.

The new technique of FLIO permits the discrimination of fluorophores according to the decay of fluorescence after pulse excitation and, to a certain degree, according to the emission spectra. Based on spectral and time-resolved *in vitro* measurements of autofluorescence on isolated structures[27]of porcine eyes and of fundi *in toto*[28] as well as of human fundus structures,[29] we assume a relation between FLIO parameters and fundus layers. Additionally, cross-sections in FLIO images also show a relation between anatomical structures and lifetimes as well as amplitudes.[30]

Thus, the amplitude α_1 and the decay time τ_1 might correspond to some extent with the retinal pigment epithelium, α_2 and τ_2 likely correspond to the neuronal retina, and α_3 and τ_3 likely demonstrate the influence of connective tissue and of the lens.

The decay times and the amplitudes in the short-wavelength channel (490 to 560 nm) differ from those in the long-wavelength channel (560 to 700 nm); thus, different substances contribute to the total fluorescence in the two channels.

In particular, the long fluorescence decay of the crystalline lens is present in the short-wavelength channel, where the τ_3 is much longer than the τ_3 in the long-wavelength channel. This contribution is confirmed because the τ_3 in the short-wavelength channel in pseudophakic eyes is much shorter than that in eyes with a crystalline lens.

To investigate such metabolic alterations, diabetic patients who have no signs of DR and age-matched healthy subjects were investigated by FLIO. Although the mean duration of diabetes mellitus was 15 years, the mean HbA1c value was $7.1 \pm 1.4\%$, which is in the 6.5 to 7.5% range recommended by the EASD/ADA[31] and by the National German Guideline.[32]

In contrast to optical coherence tomography measurements of the fundus layers and visible changes in the retinal vessel system, FLIO measurements detect functional metabolic changes.

Considering amplitudes and lifetimes after a three-exponential fit of fluorescence decay in fields of 71×101 pixels, the best discriminating parameters were the median and mean in histograms of τ_2. Because τ_2 presumably corresponds to the neuronal retina, metabolic alterations in this anatomical structure might be assumed to occur in the fundus of diabetic patients before DR is detectable in color fundus photographs. Early alterations in the vessel system are detectable by fluorescein angiography. As this is an invasive test, it was not applied for ethical reasons in people who have had no visual complaints.

In addition to the statistical evaluation of the distribution of individual FLIO parameters, the sum of the individual histograms of the amplitudes, decay times, and relative contributions was considered for both groups. Similar to each individual histogram, the sum histograms contain the fluorescence of several

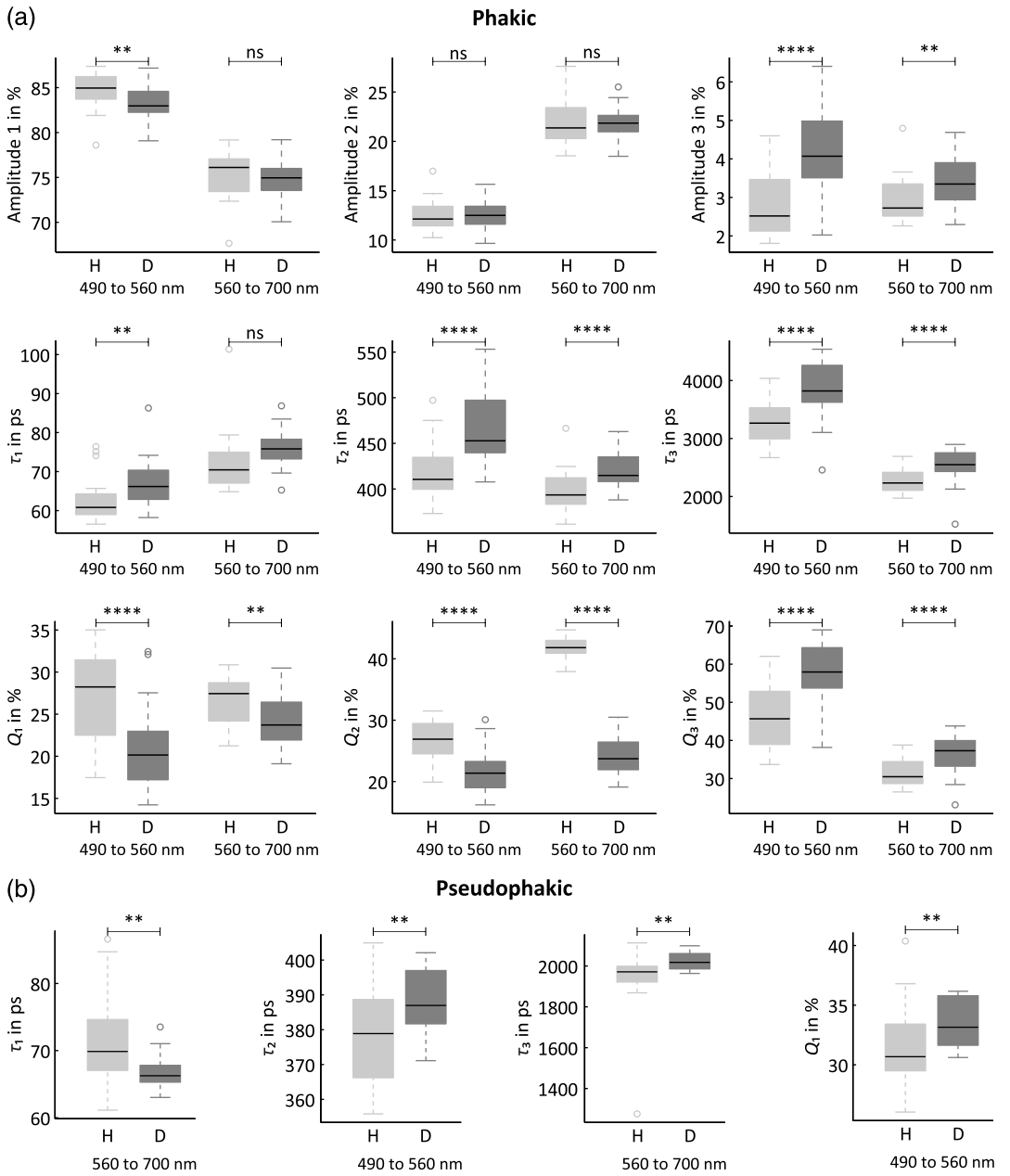

Fig. 4 Comparison of the median boxplots of different parameters between diabetic patients and healthy subjects: (a) crystalline lens, (b) intraocular artificial lens. H, healthy subjects (light gray); D, diabetic patients (dark gray); ns, not significant; $****$ $p < 0.0001$, $**$ $p < 0.05$.

fluorophores. Thus, it is difficult to attribute any alterations to changes of only one fluorophore.

Calculations of the difference between the sum histogram of diabetic patients and that of healthy subjects revealed decreased abundance at ~380 ps for τ_2 and at ~3000 ps for τ_3; however, more pixels had longer τ_2 decay times of ~480 ps and a longer τ_3 of >3800 ps.

There are several possibilities for interpretation of this change. A change in the composition of elastin (lifetime $\tau_1 =$ 380 ps/amplitude $\alpha_1 = 72\%$ and $\tau_2 = 3.59$ ns/amplitude $\alpha_2 = 28\%$) would be thinkable, in principle. But we found no hints for such changes of elastin in diabetes in the literature.

More relevant is the interpretation in connection with the underlying chemical species. The decay time of 380 ps corresponds to free NADH; thus, a lack of free NADH versus protein-bound NADH, which has decay times of several nanoseconds, can be assumed.[33] The increased contribution of protein-bound NADH is indicated by the longer τ_3 decay time and by the increased amplitude α_3 in the short-wavelength channel. This reason for the changed lifetime is unlikely because the maximal excitation of NADH is at 340 nm and the emission maximum is at 460 nm. In earlier studies,[17,20] we excited pure NADH at 446 nm and detected a weak fluorescence with a maximum at 530 nm. Because it was unlikely to excite NADH at such long wavelength, we interpreted this fluorescence as result of pollution.[17,34] Apparently, the minimal contribution of the NADH fluorescence can be detected by the highly sensitive TCSPC technique.

Table 7 Results of the Holm–Bonferroni test for diabetic patients who have no signs of DR and for healthy subjects.

Fit parameter		Significance	ROC	Sensitivity	Specificity	Best separation	Further separation intervals
Channel 490 to 560 nm	α_1	ns	0.7	0.622	0.8	82	
	α_3	0.001	0.73	0.946	0.52	1.5	1.5, 5.5
	τ_1	0.001	0.8	0.811	0.64	70	
	τ_2	0.001	0.86	0.838	0.84	400	400, 410, 480 to 580
	τ_3	0.001	0.84	0.757	0.84	3050	2800 to 3100, 4400
	τ_m	0.01	0.77	0.838	0.64	150	140 to 160, 270, 330 to 360
	Q_1	0.001	0.77	0.891	0.64	34	34 to 36
	Q_2	0.001	0.85	0.892	0.72	29	21, 28 to 31
	Q_3	0.001	0.78	0.838	0.72	40	38 to 40
Channel 560 to 700 nm	α_1	ns	0.65	0.649	0.68	74	
	α_2	ns	0.63	0.757	0.64	23	
	α_3	0.05	0.71	0.568	0.84	4.5	4 to 5
	τ_1	0.01	0.77	0.676	0.76	65	65, 80
	τ_2	0.01	0.79	0.676	0.8	450	37 to 380, 430 to 460
	τ_3	0.001	0.85	0.892	0.8	2100	2050 to 2150, 2650 to 2900
	τ_m	0.01	0.73	0.913	0.56	160	160
	Q_1	0.05	0.7	0.541	0.88	18	18, 20
	Q_2	0.001	0.87	0.757	0.96	43	35 to 39, 43 to 45
	Q_3	0.01	0.76	0.757	0.76	40	40 to 44

Table 8 Results of the Holm-Bonferroni test for pseudophakic diabetic patients who have no signs of DR and for healthy subjects.

Fit parameter		Significance	ROC	Sensitivity	Specificity	Separation interval
Channel 490 to 560 nm	α_2	ns	0.7	0.7	0.696	15
	τ_1	0.05	0.81	0.8	0.696	65
	τ_2	ns	0.73	0.7	0.652	410
	τ_3	ns	0.76	0.7	0.739	2500
	τ_m	ns	0.72	0.6	0.739	140
	Q_3	ns	0.8	0.7	0.826	26
Channel 560 to 700 nm	τ_1	ns	0.71	0.9	0.565	85
	τ_2	ns	0.72	0.8	0.652	410
	τ_3	ns	0.79	0.9	0.652	2100
	Q_3	ns	0.72	0.8	0.652	28

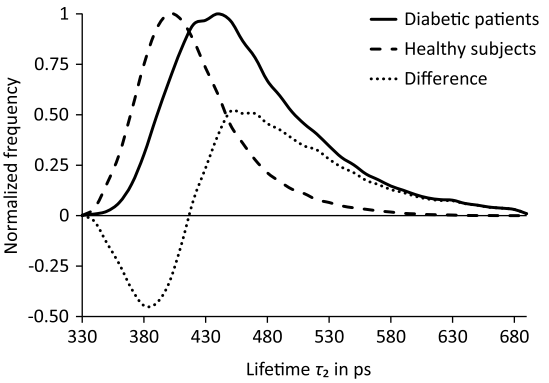

Fig. 5 Sum and difference histograms of lifetime τ_2 in the short-wavelength channel (490 to 560 nm).

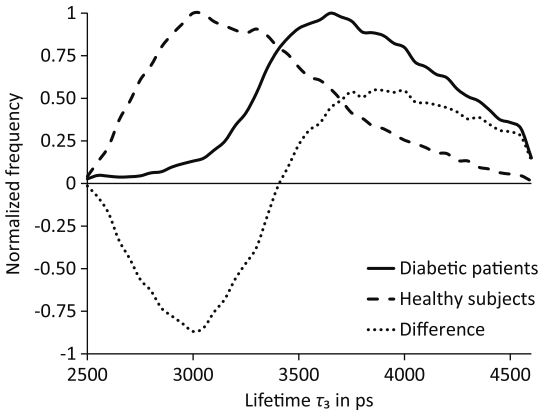

Fig. 6 Sum and difference histograms of lifetime τ_3 in the short-wavelength channel (490 to 560 nm).

A shift of NADH from the free to the protein-bound state results from an increased contribution of glycolysis to energy production.[35]

The elongated fluorescence lifetime τ_2 in diabetic subjects, especially in the short-wavelengths channel, is most likely interpretable as an increased contribution of free FAD. Field et al.[12] published an increased fluorescence intensity of FAD in diabetic eyes. The applied excitation wavelength and emission range are optimally suited for detection of FAD. In our own measurements, we found the lifetimes of free FAD using a biexponential fit to be $\tau_1 = 330$ ps with $\alpha_1 = 18\%$ and $\tau_2 = 2810$ ps with $\alpha 2 = 82\%$.[17] The lifetime of protein-bound FAD is 100 ps.[36]

Though the number of subjects with an artificial lens is low, the results of these groups demonstrate the influence of the fluorescence of the crystalline lens. This fluorescence contributes to the fluorescence that is detected from the eye. The confocal detection principle only reduces the contribution of the fluorescence of the lens, but does not avoid it completely.[37] As the excited volume of the lens is much higher in fundus cameras, using the principle of aperture separation, the contribution of fluorescence of the lens cannot be neglected in fluorescence measurements of the eye. Thus, diabetic metabolic changes can be assumed, which accumulate in the crystalline lens, too. As mitochondria are missing in the lens, the accumulation of AGEs can be assumed in the lens. In in-house measurements, AGEs were excited at 446 nm and emit with a maximum at 520 nm. The corresponding lifetimes using a biexponential fit were $\tau_1 = 865$ ps with $\alpha_1 = 62\%$ and $\tau_2 = 4170$ ps with $\alpha_2 = 28\%$.[17]

Considering all these aspects, the detected changes in the time-resolved autofluorescence in type 2 diabetes are the result of several metabolic alterations, most probably the accumulation of AGEs in the lens and the production of free FAD and accumulation of AGEs in the neuronal retina at the fundus. A change from free to protein-bound NADH cannot completely be excluded.

In conclusion, FLIO is a promising new method for investigation of the metabolism of the eye based on fluorescence lifetime of endogenous fluorophores. To get information about the fundus fluorescence alone, the fluorescence decay of the lens should be measured separately and be used in the fit of the fluorescence decay, detected from the whole eye. To specify the interpretation of metabolic alterations, techniques should be developed, permitting FLIO measurements in single fundus layers of the living human eye.

Acknowledgments

This research was supported by the German Federal Ministry of Education and Research (Grant No. 03IPT605A) and the German Research Council (DFG HA 2899/19-1).

References

1. Y. Ohkubo et al., "Intensive insulin therapy prevents the progression of diabetic microvascular complications in Japanese patients with non-insulin dependent diabetes mellitus: a randomized prospective 5-year study," *Diab. Res. Clin. Pract.* **28**, 103–117 (1995).
2. UK Prospektive Diabetes Study (UKPDS) Group, "Intensive blood-glucose control with sulfonyl ureas or insulin compared with conventional treatment and risk of complications in patients with type 2 diabetes (UKPDS 33)," *Lancet* **352**, 837–853 (1998).
3. A. J. Barber, T. W. Gardner, and S. F. Abcouwer, "The significance of vascular and neural apoptosis to the pathology of diabetic retinopathy," *Invest. Ophthalmol. Vis. Sci.* **52**, 1156–1162 (2011).
4. A. J. Barber et al., "Neural apoptosis in the retina during experimental and human diabetes: early onset and effect of insulin," *J. Clin. Invest.* **102**, 783–791 (1998).
5. A. B. El-Remessy et al., "Neuroprotective and blood-retinal barrier-preserving effect of cannabitol in experimental diabetes," *Am. J. Pathol.* **168**, 235–244 (2006).
6. R. M. H. Diederen et al., "Reexamining the hyperglycemic pseudohypoxia hypothesis of diabetic oculopathy," *Invest. Ophthalmol. Vis. Sci.* **47**, 2726–2731 (2006).
7. M. S. Ola et al., "Analysis of glucose metabolism in diabetic rat retinas," *Am. J. Physiol. Endocrinol. Metab.* **290**, E1057–E1067 (2006).
8. Y. Ido et al., "Early neural and vascular dysfunction in diabetic rats are largely sequelae of increased sorbitol oxidation," *Antioxid. Redox Signal.* **12**, 39–51 (2010).
9. E. Lieth et al., "Retinal neurodegeneration: early pathology in diabetes," *Clin. Exp. Ophthalmol.* **28**, 3–8 (2000).
10. J. H. Yang et al., "Retinal neurodegeneration in type II diabetic Otsuka Long-Evans Tokusshima fatty rats," *Invest. Ophthalmol. Vis. Sci.* **54**, 3844–3851 (2013).
11. R. U. Kowluru and S. N. Abbas, "Diabetes-induced mitochondrial dysfunction in the retina," *Invest. Ophthalmol. Vis. Sci.* **44**, 5327–5334 (2003).
12. M. G. Field et al., "Rapid, noninvasive detection of diabetes-induced retinal metabolic stress," *Arch. Ophthalmol.* **126**(7), 934–938 (2008).
13. F. C. Delori et al., "In vivo fluorescence of the ocular fundus exhibits retinal pigment epithelium lipofuscin characteristics," *Invest. Ophthalmol. Vis. Sci.* **36**(3), 718–729 (1995).
14. D. Schweitzer, "Ophthalmic applications of FLIM," Chapter 20 in *Fluorescence Lifetime Spectroscopy and Imaging*, L. Marcu, P. M. W. French, and D. S. Elson, Eds., pp. 423–447, CRC Press, Boca Raton, FL (2014).

15. Early Treatment Diabetic Retinopathy Study Research Group., "Grading diabetic retinopathy from stereoscopic color fundus photographs—an extension of the modified Airlie House classification. ETDRS report number 10," *Ophthalmology* **98**, 786–806 (1991).
16. H. W. van Dijk et al., "Early neurodegeneration in the retina of type 2 diabetic patients," *Invest. Ophthalmol. Vis. Sci.* **53**, 2715–2719 (2012).
17. D. Schweitzer et al., "Towards metabolic mapping of the human retina," *Microsc. Res. Tech.* **70**, 410–419 (2007).
18. D. Schweitzer, "Quantifying fundus autofluorescence," Chapter 8 in *Fundus Autofluorescence*, N. Lois and J. V. Forrester, Eds., pp. 78–95, Wolters Kluwer Lippincott Williams & Wilkins, Philadelphia, PA (2009).
19. E. Y. Chew et al., "Evaluation of the age-related eye disease study clinical lens grading system AREDS report no. 31," *Ophthalmology* **117**, 2112–2119 (2010).
20. L. Deutsch, "Evaluierung des Fluorescence Lifetime Imaging vom Augenhintergrund bei Patienten mit Diabetes mellitus," MD Dissertation, FSU Jena, Germany (2012).
21. C. Dysli et al., "Quantitative analysis of fluorescence lifetime measurements of the macula using the fluorescence lifetime imaging ophthalmoscope in healthy subjects," *Invest. Ophthalmol. Vis. Sci.* **55**, 2106–2113 (2014).
22. C. Kloos et al., "Unnoticed shift in the normal range of glycated HbA1c with TOSOH high performance liquid chromatography," *Diabetologia* **54**(Suppl. 1), 401 (2011).
23. Diabetes Control and Complication Trial Research Group, "The effect of intensive treatment of diabetes on the development and progression of long-term complications in insulin-dependent diabetes mellitus," *N. Engl. J. Med.* **329**, 977–986 (1993).
24. S. Holm, "A simple sequentially rejective multiple test procedure," *Scand. J. Stat.* **6**, 65–70 (1979).
25. M. Klemm, private communication, University of Technology, Institute of Biomedical Engineering and Informatics, Ilmenau, Germany (2010).
26. M. Klemm et al., "Repeatability of autofluorescence lifetime imaging at the human fundus in healthy volunteers," *Curr. Eye Res.* **38**, 793–801 (2013).
27. D. Schweitzer et al., "Spectral and time-resolved studies on ocular structures," *Proc. SPIE* **6628**, 662807 (2007).
28. S. Peters, M. Hammer, and D. Schweitzer, "Two-photon excited fluorescence microscopy application for ex vivo investigation of ocular fundus samples," *Proc. SPIE* **8086**, 808605 (2011).
29. D. Schweitzer et al., "Time-resolved autofluorescence imaging of human donor retina tissue from donors with significant extramacular drusen," *Invest. Ophthalmol. Vis. Sci.* **53**, 3376–3386 (2012).
30. D. Schweitzer et al., "Detection of early metabolic alterations in the ocular fundus of diabetic patients by time-resolved autofluorescence of endogenous fluorophores," *Proc. SPIE* **8087**, 80871G (2011).
31. S. E. Inzucchi et al., "Management of hyperglycemia in type 2 diabetes: a patient-centered approach: position statement of the American Diabetes Association (ADA) and the European Association for the Study of Diabetes (EASD)," *Diabetes Care* **35**, 1364–1379 (2012).
32. H. H. Abholz et al., "Nationale Versorgungs Leitlinie Therapie des Typ-2 diabetes," *Dtsch. Arztebl.* **110**(40), A-1875/B-1655/C-1623 (2013).
33. H. D. Vishwasrao et al., "Conformational dependence of intracellular NADH on metabolic state revealed by associated fluorescence anisotrophy," *J. Biol. Chem.* **280**, 25119–25126 (2005).
34. D. Schweitzer, "Metabolic mapping," Chapter 10 in *Medical Retina*, F. G. Holz and R. F. Spaide, Eds., pp. 107–123, Springer, Berlin Heidelberg (2010).
35. V. Jyothikumar, Y. Sun, and A. Periasamy, "Investigation of tryptophan–NADH interactions in live human cells using three-photon fluorescence lifetime imaging and Förster resonance energy transfer microscopy," *J. Biomed. Opt.* **18**, 060501 (2013).
36. M. C. Skala et al., "In vivo multiphoton microscopy of NADH and FAD redox states, fluorescence lifetimes, and cellular morphology in precancerous epithelia," *PNAS* **104**(49) 19494–19499 (2007).
37. D. Schweitzer, M. Hammer, and F. Schweitzer, "Limitations of the confocal laser scanning technique in measurements of time-resolved autofluorescence of the ocular fundus," *Biomed. Tech. (Berl.)* **50**, 263–267 (2005).

Dietrich Schweitzer received his Dipl.-Ing. in 1967, Dr.-Ing. in 1976, and the habilitation degree in 1990 from the Technical University of Ilmenau, Germany. From 1979, he was with the University of Jena, Germany, and was the head of experimental ophthalmology (EO) until his retirement in 2008. In 1995, he was appointed to a docent of EO. He developed a method for measuring the oxygen saturation, the optical density of xanthophyll, and was the founder of FLIO.

Lydia Deutsch: Biography is not available.

Matthias Klemm received his master's degree in biomedical engineering from the Technische Universität Ilmenau. He is currently involved in the development of new methods for the analysis of time-resolved fluorescence data from the human eye. Present interests also include electrical current stimulation of the human eye and dynamic vessel analysis.

Susanne Jentsch has worked as a scientist in the Jena University Hospital, Department of Ophthalmology, since 2007. After receiving a graduate degree of optometry and vision science in 2007 at the ERNST-ABBE-University of Applied Science in Jena, she worked on clinical-experimental studies with focus on macular pigment density in age-dependent macular degeneration (AMD) as well as fluorescence lifetime imaging in AMD, glaucoma and Alzheimer 's disease.

Martin Hammer studied physics at the University of Jena and received his diploma degree in 1983 and his PhD in 1998. From 1983 to 1990, he was with Carl Zeiss Jena. Since 1990, he has been with the University of Jena, Department of Ophthalmology. Currently, he is head of the experimental ophthalmology group. His recent research interests are functional imaging of the ocular fundus, retinal blood flow and oximetry, as well as autofluorescence lifetime imaging.

Sven Peters studied biochemistry at the University of Jena and received his diploma in 2005. Since he started his PhD he has been fascinated working with fluorescence lifetime imaging. Using this technique he investigated protein-protein interactions on microarrays at the Institute of Photonic Technology Jena. In 2010 he joined the experimental ophthalmology group at the University Hospital Jena and focuses now on early diagnostics of retinal disorders, using autofluorescence lifetime and anisotropy imaging.

Jens Haueisen received his MS in 1992 and his PhD in 1996 in electrical engineering from the Technical University Ilmenau. From 1998 to 2005, he was the head of the Biomagnetic Center, Friedrich-Schiller-University, Jena, Germany. Since 2005, he has been a professor of biomedical engineering and directs the Institute of Biomedical Engineering and Informatics at the Technical University Ilmenau. His research interests include the investigation of active and passive bioelectric and biomagnetic phenomena and medical technology for ophthalmology.

Ulrich A. Müller studied medicine from 1974 to 1980 at the University of Jena. He graduated in 1982 with a degree in pathological anatomy, in 1995 as Doctor habilitatus in diabetology, and in 1993 with a Master of Science in clinical biochemistry from the University of Aberdeen. In 2002, he was professor of internal medicine, and in 2003 head of the Department of Endocrinology and Metabolic Diseases at University Hospital Jena, Germany. He has done studies on diabetes health care delivery, diabetic late complication, insulin therapy, patient education.

Jens Dawczynski studied medicine from 1990 to 2001 at the University of Jena. He received his MD in 2001 and habilitation degree and postdoctoral lecture qualification in ophthalmology in 2008. In 2011, he was appointed as professor of fundus imaging at University of Leipzig, Department of Ophthalmology. He has been the associate director and senior physician in this department. He leads studies on diabetic retinopathy, retinal vessel occlusion, and age-related macular degeneration.